J Therm Anal Calorim (2012) 109:33–38
DOI 10.1007/s10973-011-1527-4

Synthesis of Sr-doped $LaCrO_3$ powders by combustion method

Influence of the fuel agent

Adney Luís A. da Silva · Guilherme G. G. Castro · Mariana M. V. M. Souza

Received: 19 November 2010 / Accepted: 23 March 2011 / Published online: 8 April 2011

Abstract Lanthanum strontium chromite (LSC) powders were synthesized by the combustion method, using five different fuels (urea, glycine, ethylene glycol, α-alanine, and citric acid). The ignition of the reagent mixture with urea takes a longer time, and more gases are released by combustion. A calcination step is essential for a good crystallization of the perovskite phase. X-ray diffraction patterns showed formation of perovskite phase and a small amount of $SrCrO_4$ for the sample synthesized with urea after calcination. The crystallite sizes are in the range of 23–33 nm. Scanning electron microscopy revealed the porosity of the powders and the presence of agglomerates, formed by fine particles of different shapes. Thermogravimetric analysis showed a large mass loss for the sample synthesized with citric acid, probably caused by the absence of ignition, with primary polymerization of the precursor reagents.

Keywords Doped lanthanum chromites · Combustion synthesis · Flame temperature · X-ray diffraction

Introduction

Perovskites are mixed ceramic oxides with ABO_3-type crystal structure where cations with a large ionic radius have 12 coordination to oxygen atoms and occupy A-sites, and cations with smaller ionic radius have 6 coordination and occupy B-sites [1]. A and O form a cubic packing, and B is contained in the octahedral voids in the packing. The perovskite structure may undergo atomic distortion leading to orthorhombic or rhombohedral unit cells [2].

Perovskite-like lanthanum chromites are interesting materials for application in solid oxide fuel cells (SOFCs) due to chemical and thermal stability, mechanical strength, and high electrical conductivity [2, 3]. The electrical conductivity of these materials can be enhanced by substituting a lower valence ion, such as Sr, on the La site. Sr-doped $LaCrO_3$ (LSC) is currently the preferred material for interconnect in SOFC [3, 4].

Different synthesis methods have been developed for the production of perovskite powders, like solid-state reaction, sol–gel technique, hydrothermal synthesis, co-precipitation, and combustion [5–8]. Combustion synthesis is characterized by fast heating rates, high temperatures, and short reaction times [9, 10]. It is a straightforward preparation process to produce homogeneous, very fine, crystalline, and unagglomerated multicomponent oxide powders, without intermediate decomposition steps [11]. In the solution combustion synthesis, an aqueous solution of the desired metal salts is heated together with a suitable organic fuel, until the mixture ignites and a fast combustion reaction takes off [9, 12].

Various fuels have been used in the combustion synthesis of perovskites, like glycine, urea, oxalyl-hydrazine, citric acid, and sucrose [8, 13–15]. All these fuels serve two purposes: (i) they are the source of C and H, the reducing elements, which form CO_2 and H_2O on combustion and liberate heat; and (ii) they form complexes with the metal ions facilitating homogeneous mixing of the cations in solution [9]. The fuels differ in the reducing power, the combustion temperature, and the amount of gases they generate, which affects the characteristics of the reaction product [12]. The properties of ceramic materials for

A. L. A. da Silva · G. G. G. Castro · M. M. V. M. Souza (✉)
Escola de Química—Universidade Federal do Rio de Janeiro (UFRJ), Centro de Tecnologia, Bloco E, sala 206, Rio de Janeiro, RJ CEP 21941-909, Brazil
e-mail: mmattos@eq.ufrj.br

electrodes in SOFC are extremely dependent on the conditions of powder synthesis, which in turn depend on the nature of the fuel used in the combustion synthesis.

Mukasyan et al. [16] and Deshpande et al. [17] showed that the mechanism of combustion synthesis of LSC and the characteristics of the synthesized powders are closely related to the glycine/oxidizer ratio; increasing this ratio the flame temperature increases. The mechanism of combustion synthesis of lanthanum chromite with urea was investigated by Biamino and Badini [18] using thermal analysis and identifying reaction products by mass spectrometry. To the best of our knowledge, none of the combustion synthesis studies until now reported the effect of the fuel on the structural and morphological properties of LSC powders.

The aim of this work is to study the influence of the fuel used in the combustion synthesis on the flame temperature and ignition time of lanthanum strontium chromite (LSC) powders. The combustion synthesized powders were characterized by X-ray diffraction (XRD), scanning electron microscopy (SEM), and Thermogravimetric analysis/differential thermal analysis (TG/DTA), analyzing the variation in the powder properties based on the characteristics of combustion reaction.

Experimental

Material synthesis

The materials used in the synthesis were metal nitrates: $La(NO_3)_3{\cdot}6H_2O$, $Sr(NO_3)_2$, $Cr(NO_3)_3{\cdot}9H_2O$, and the propellants were citric acid ($C_6H_8O_7$), α-alanine ($CH_3CH(NH_2)COOH$), ethylene glycol ($C_2H_6O_2$), glycine (NH_2CH_2COOH), and urea ($CO(NH_2)_2$). All reagents were from VETEC, Brazil, with purity of 99.9%.

The samples were synthesized by combustion method, where the metal nitrates were dissolved with the fuel in distilled water and heated (under stirring) at 80 °C, until the water evaporation and formation of a gel. After that, the gel was introduced in a muffle furnace (EDG 3000 3P), previously heated at 300 °C. Once ignited, the gel underwent a combustion process and yielded a voluminous powder. The ignition time and the flame temperature were measured during the combustion synthesis, with a thermocouple (type K) inserted in the reagent mixture. The powder was then calcined in flowing air (60 mL min^{-1}) with a heating rate of 10 °C min^{-1} up to 900 °C for 6 h.

The amount of fuel used on the preparation of these materials was based on the following equation: $\Sigma n_i{\cdot}v_i = 0$, where n_i is the number of moles of each reagent and v_i is the number of oxidation, calculated according to the propellant chemistry [19]. The fuel/oxidizer (metal nitrates) ratio corresponds to the stoichiometric ratio. The combustion reactions can be expressed as follows:

$$0.7La(NO_3)_3{\cdot}6H_2O + 0.3Sr(NO_3)_2 + Cr(NO_3)_3{\cdot}9H_2O + 1.57C_6H_8O_7 \rightarrow La_{0.7}Sr_{0.3}CrO_3 + 2.85N_2 + 19.47H_2O + 9.4CO_2$$

$$0.7La(NO_3)_3{\cdot}6H_2O + 0.3Sr(NO_3)_2 + Cr(NO_3)_3{\cdot}9H_2O + 1.88C_3H_7NO_2 \rightarrow La_{0.7}Sr_{0.3}CrO_3 + 3.79N_2 + 19.78H_2O + 5.64CO_2$$

$$0.7La(NO_3)_3{\cdot}6H_2O + 0.3Sr(NO_3)_2 + Cr(NO_3)_3{\cdot}9H_2O + 2.82C_2H_6O_2 \rightarrow La_{0.7}Sr_{0.3}CrO_3 + 2.85N_2 + 21.66H_2O + 5.64CO_2$$

$$0.7\ La(NO_3)_3{\cdot}6H_2O + 0.3Sr(NO_3)_2 + Cr(NO_3)_3{\cdot}9H_2O + 3.17C_2H_5NO_2 \rightarrow La_{0.7}Sr_{0.3}CrO_3 + 4.44N_2 + 21.13H_2O + 6.34CO_2$$

$$0.7La(NO_3)_3{\cdot}6H_2O + 0.3Sr(NO_3)_2 + Cr(NO_3)_3{\cdot}9H_2O + 4.75(NH_2)_2CO \rightarrow La_{0.7}Sr_{0.3}CrO_3 + 7.60N_2 + 22.70H_2O + 4.75CO_2$$

All $La_{1-x}Sr_xCrO_3$ powder materials were prepared with nominal composition of $x = 0.3$. The prepared perovskites will be identified according with the fuel agent: LSCC (citric acid), LSCA (alanine), LSCE (ethylene glycol), LSCG (glycine), and LSCU (urea).

Characterization

X-ray powder diffraction (XRD) patterns were recorded in a Rigaku Miniflex II diffractometer, with CuKα radiation and monochromator, with speed of 2°min^{-1}. The crystallite sizes (D_{XRD}) and microstrain (ε) of the calcined samples were calculated using the model proposed by Williamson and Hall [20], by means of the following formula:

$$\beta\cos\theta/\lambda = 1/D_{XRD} + 4\varepsilon\sin\theta/\lambda \quad (4)$$

where θ is the diffraction angle, λ is the wavelength of incident radiation, and β is the full width at half maximum (FWHM) of the peak. Plotting the $\beta\cos\theta/\lambda$ versus $4\sin\theta/\lambda$, straight line yields the crystallite size from interception with the ordinate and microstrain from the slope. The calculus was done using the FullProf software.

The microstructure of the powders was investigated by SEM using Hitachi TM-1000 equipment. The acceleration voltage was 15 kV using backscattering electron.

Thermogravimetric analysis and differential thermal analysis of the as-prepared powders were carried out using a TA thermal analyzer (SDT Q600 model) with heating

rate of 10 °C min^{-1} in air flow (100 mL min^{-1}) from room temperature up to 1000 °C.

Results and discussion

Time and temperature of combustion reaction

Figure 1 shows the evolution of temperature as a function of time during the combustion synthesis, according with the fuel agent. For all the samples, except for the citric acid, the reaction has an ignition time with a rapid increase of temperature in a short time, showing the occurrence of the combustion process. For the sample synthesized with citric acid, the increase of temperature is very small and slow, without a visible combustion, which indicates the poor quality of this fuel for combustion synthesis.

The ignition time and the maximum flame temperature for the synthesized samples are shown in Table 1. The ignition of the reagent mixture with urea takes a longer time, and the maximum temperature is 471 °C, lower than glycine and alanine. The combustion process with alanine is relatively fast, attaining the highest flame temperature (528 °C). The combustion process with ethylene glycol is extremely fast (only 7 s for ignition), with smaller flame temperature. As ethylene glycol is the only liquid fuel, the low temperature can be associated with an evaporation of fuel during the initial heating, causing a small lost of the reagent. The combustion process with glycine is intermediate between alanine and urea.

The properties of reagents are a key factor for understanding the combustion process. Table 2 shows some properties of the fuels. Citric acid has low heat of combustion, which may be correlated with the absence of ignition. On the other hand, alanine has the highest heat of combustion, and this explains the high flame temperature achieved in this study. Hwang et al. [21] also showed that

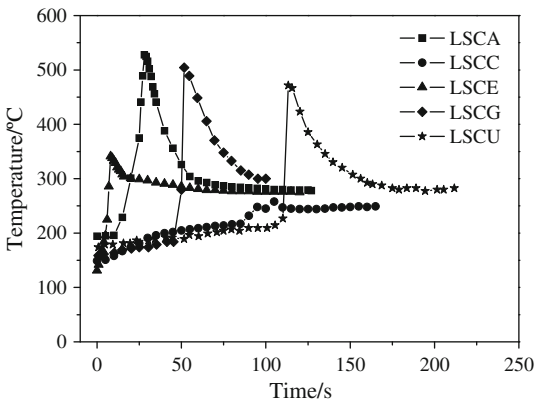

Fig. 1 Evolution of temperature as a function of time during the combustion synthesis

Table 1 Ignition time and maximum flame temperature for each sample

Sample	Ignition time/s	Maximum flame temperature/°C
LSCA	29	528
LSCC	–	258
LSCE	7	341
LSCG	51	508
LSCU	113	471

glycine has a higher melting point and its heat of combustion is higher than that of urea, which may be contributing for a less complete combustion when glycine is compared to urea, as will be shown by TG profiles later.

The temperature profiles show that urea favors a more complete combustion reaction during the synthesis process, with evolution of a larger amount of gases, which contributes to the formation of materials of high porosity, good crystallinity and nanometric particles [22].

Deshpande et al. [17] measured a maximum reaction temperature of 806 °C for LSC prepared by combustion with glycine, and the complete conversion occurred in only 10 s, when using a fuel/oxidizer ratio between 0.7 and 1.2. The temperatures measured in this study (with fuel/oxidizer ratio = 1) were lower than those reported by Deshpande et al. [17], which can be related to inhomogeneous precursor mixture and higher dissipation of heat, with a longer time of reaction. On the other hand, Civera et al. [23] observed no visible reaction during combustion synthesis of $LaMnO_3$ using stoichiometric conditions with urea. Thus, the measurement of the combustion temperature is highly sensitive to the specific conditions employed by each group.

Phase formation and microstructure

Figure 2 shows the XRD patterns of the prepared samples. Before calcination (Fig. 2a), there was no formation of perovskite phase for the samples synthesized with citric acid and ethylene glycol. This can be explained by the low temperature reached by these samples during the combustion synthesis, showing the importance of choice of the appropriated fuel agent. Samples prepared from glycine and alanine showed a partial formation of the perovskite phase, and a good crystallization of LSC can be observed for the sample prepared with urea.

After calcination (Fig. 2b) the presence of secondary phases decreased significantly, showing that calcination is an essential step for a good crystallization of perovskite phase. This result agrees with Muskasyan et al. [16] who pointed out the need of a calcination step for the

Table 2 Some properties of the utilized fuel agents

Properties	Fuel agents				
	α-alanine	glycine	Ethylene glycol	Urea	Citric acid
Molar mass/g mol^{-1}	89.1	75.1	62.1	60.1	192.1
Heat of combustion/kJ g^{-1}	18.2	13.0	17.0	10.5	9.3
Melting point/°C	258	232	−12.9	135	153

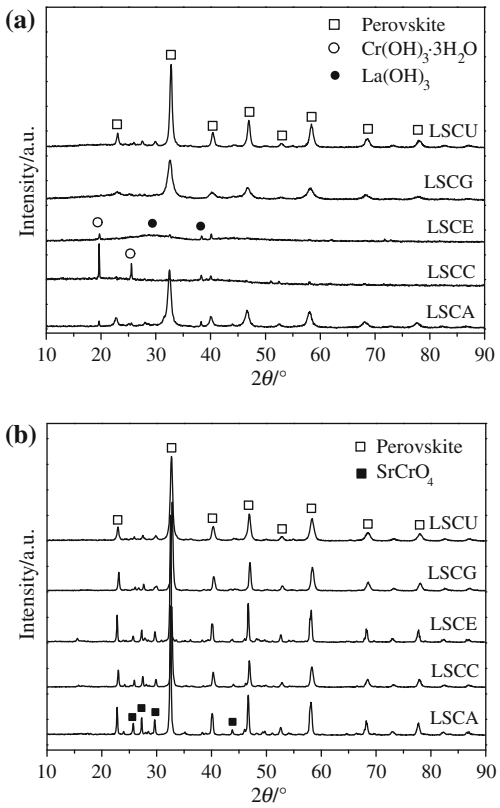

Fig. 2 XRD patterns of the LSC powders before (**a**) and after (**b**) calcination

as-synthesized LSC powders to remove residual water and other volatile components and to improve the crystalline structure of the powder. It is important to note that the calcination temperature used here (900 °C) is much lower than that used for LSC synthesized by the conventional solid-state reaction: 1200 [24, 25] or even 1400 °C [26].

The combustion reaction with urea is far more complete, resulting in a crystalline material with almost single LSC phase (JCPDS 321240), with a small contribution of secondary phase of $SrCrO_4$ (JCPDS 350743). The chromate phase is much more significant in the samples derived from alanine, citric acid, and ethylene glycol, as confirmed by Rietveld refinement: for alanine it reaches 6.8 wt%, while for urea sample is only 2.5%. This secondary phase was also observed for LSC prepared from combustion with urea by Marinho et al. [27] and with citric acid by Zupan et al. [28].

Table 3 shows the microstrain and crystallite sizes calculated from XRD data using the Williamson–Hall equation and the lattice parameters. All products obtained in this study were nanocrystalline with sizes ranging between 23.2 and 33.1 nm. Broad XRD peaks indicate the nanocrystalline nature of the synthesized powders with little lattice distortions, since the values of microstrain are very low. It is worth noting that the crystallite sizes obtained by the combustion method are much smaller than those obtained by other methods, as reported by Rida et al. [29] for $LaCrO_3$ prepared by sol–gel synthesis and calcined at 800 °C (179 nm).

The smaller crystallite size was formed when using urea because the large volume of gases evolved enhances dissipation of heat and limits inter-particle contact [30]. The lattice parameters calculated from XRD data are consistent with the rhombohedral structure for doped perovskites, in agreement with other literature data [15, 24].

Figure 3 shows SEM micrographs of the perovskite samples after calcination. The powders presented a spongy aspect, except for sample synthesized with citric acid, with primary particles linked together in agglomerates of different sizes and shapes, in accordance with other results of combustion synthesis in the literature [16, 29, 31]. The samples prepared with urea have higher porosity compared with the other fuel agents. The combustion reaction with urea presents a great evolution of gases, resulting in porous structures with smaller particle size. The sample synthesized with citric acid is much less porous comparing with

Table 3 Microstrain (ε), average crystallite size (D_{XRD}), and lattice parameters of the calcined samples

Sample	ε/%	D_{XRD}/nm	Lattice parameters/Å
LSCA	0.31	28.0	$a = 5.4324$; $c = 13.3509$
LSCC	0.40	33.1	$a = 5.3794$; $c = 13.2494$
LSCE	0.25	30.9	$a = 5.4182$; $c = 13.3392$
LSCG	0.24	24.9	$a = 5.6013$; $c = 13.3049$
LSCU	0.38	23.2	$a = 5.4545$; $c = 13.4174$

Theoretical cell parameters: JCPDS 321240 ($a = 5.4030$; $c = 13.3010$ Å)

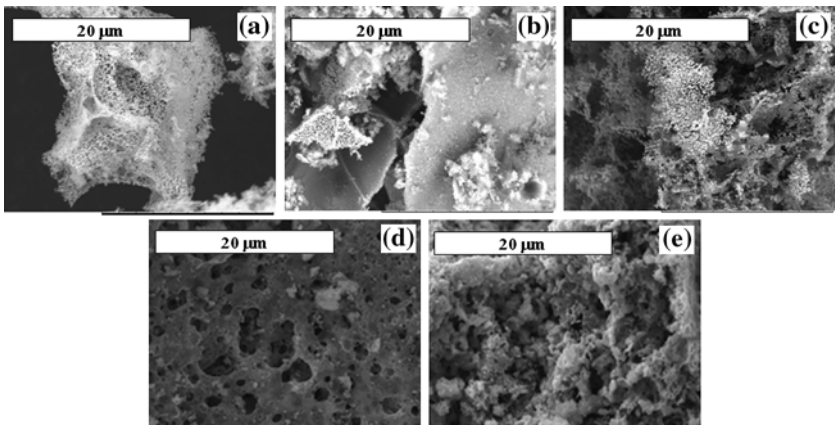

Fig. 3 Micrographs of the calcined samples: **a** LSCA; **b** LSCC; **c** LSCE; **d** LSCG, and **e** LSCU

the other samples, which can be attributed to the synthesis process. The combustion with citric acid is not effective, reaching a lower flame temperature, resulting in particles with small porosity, probably because of a primary polymerization of the precursor reagents [32].

Thermal analysis

Figure 4 shows TG curves of the as-synthesized powders. Thermal decomposition takes place in different stages, depending on the fuel, and burn out of organics is complete at about 850–900 °C for all samples.

The sample prepared with urea showed a very small mass loss (<4%), which is directly related to the slower combustion, with minor formation of organic residues. For the samples synthesized with urea, glycine, and alanine, it is difficult to distinguish between decomposition stages with a slightly continuous mass loss.

The samples synthesized with ethylene glycol and citric acid presented larger mass losses, which is associated with the incomplete combustion in the synthesis route. Particularly, the noticeable mass loss of the LSCC sample (>72%) is due to the absence of ignition and low combustion temperature with large amount of organic residues.

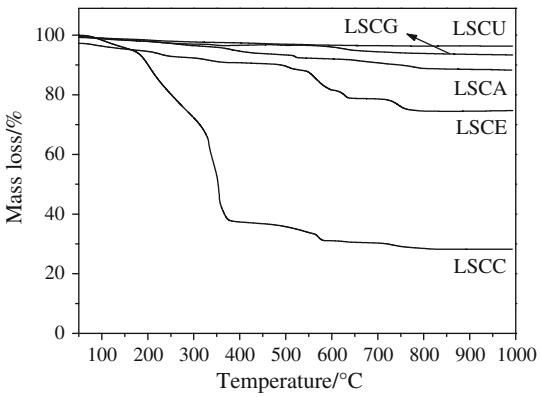

Fig. 4 TG curves of the as-synthesized samples

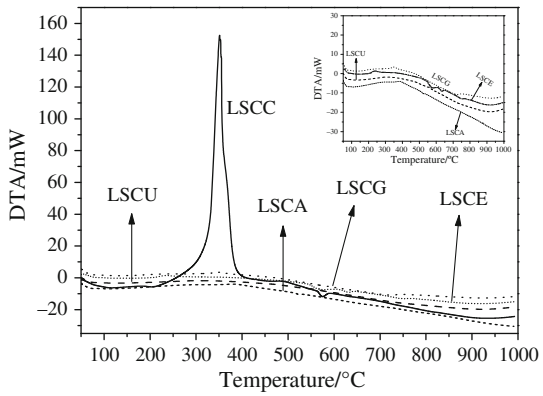

Fig. 5 DTA curves of the as-synthesized samples

For this sample three decomposition stages can be distinguished: the first, up to 200 °C, can be assigned to the desorption of physisorbed water; the second, at 200-400 °C, can be associated with the decomposition of combustion residues, mainly fuel that was not burnt during the combustion reaction; the third, at about 550-600 °C, may be due to complete dissociation of carbonates produced during combustion [30].

DTA profiles of the as-synthesized samples are displayed in Fig. 5. The sample synthesized with citric acid presented a great exothermic peak at 350 °C, associated with oxidation of the fuel agent, and a small endothermic peak at 570 °C, due to dissociation of carbonates. The other samples presented very small exothermic events at 230–350 °C, related to the oxidation of combustion residues, and LSCE also shows small endothermic peaks at 570–630 °C.

Conclusions

The combustion synthesis method from nitrate precursors has been used to prepare nanocrystalline Sr-doped chromite powders. According to our results, combustion

temperature, phase formation, crystallite size, porosity, and thermal stability are dependent on the nature of the fuel.

The samples synthesized with alanine, glycine and urea presented a more complete combustion, attaining a high flame temperature. The sample synthesized with ethylene glycol presented a less intense combustion with a smaller flame temperature. The sample prepared with citric acid did not present a combustion ignition, resulting in powder with bigger crystallite size, smaller porosity, and a large mass loss observed in TG curves due to organic residues.

All samples presented good crystallinity after calcination with small formation of secondary phase of $SrCrO_4$. The sample synthesized with urea presented better phase formation, smaller crystallite size and more porosity, due to slower combustion and more gaseous products released.

Acknowledgements The authors thank to CNPq, CAPES, and FAPERJ for financial support granted to carry out this study.

References

1. Tanaka H, Misono M. Advances in designing perovskite catalysts. Curr Opin Solid State Mater Sci. 2001;5:381–7.
2. Minh NQ. Ceramic fuel cells. J Am Ceram Soc. 1993;76:563–88.
3. Singhal SC, Kendall K. High temperature solid oxide fuel cells: fundamentals, design and applications. Oxford: Elsevier; 2004.
4. Jiang SP, Li J. Cathodes. In: Fergus JW, Hui R, Li J, Wilkinson DP, Zhang J, editors. Solid oxide fuel cells: materials, properties and performance. Boca Raton: CRC Press; 2009. p. 131–77.
5. Zhang Q, Nakagawa T, Saito F. Mechanochemical synthesis of $La_{0.7}Sr_{0.3}MnO_3$ by grinding constituent oxides. J Alloys Compd. 2000;308:121–5.
6. Bell RJ, Millar GJ, Drennan J. Influence of synthesis route on the catalytic properties of $La_{1-x}Sr_xMnO_3$. Solid State Ion. 2000;131:211–20.
7. Chick LA, Pederson LR, Maupin GD, Bates JL, Thomas LE, Exarhos GJ. Glycine-nitrate combustion synthesis of oxide ceramic powders. Mater Lett. 1990;10:6–12.
8. Yang YJ, Wen T-L, Tu H, Wang D-Q, Yang J. Characteristics of lanthanum strontium chromite prepared by glycine nitrate process. Solid State Ion. 2000;135:475–9.
9. Patil KC, Aruna ST, Mimani T. Combustion synthesis: an update. Curr Opin Solid State Mater Sci. 2002;6:507–12.
10. Varma A, Rogachev AS, Mukasyan AS, Hwang S. Combustion synthesis of advanced materials: principles and applications. Adv Chem Eng. 1998;24:79–226.
11. Segadães AM, Morelli MR, Kiminami RGA. Combustion synthesis of aluminium titanate. J Eur Ceram Soc. 1988;18:771–81.
12. Fumo DA, Jurado JR, Segadães AM, Frade JR. Combustion synthesis of iron-substituted strontium titanate perovskites. Mater Res Bull. 1997;32:1459–70.
13. Prabhakaran K, Joseph J, Gokhale NM, Sharma SC, Lal R. Sucrose combustion synthesis of $La_xSr_{(1-x)}MnO_3$ ($x \leq 0.2$) powders. Ceram Int. 2005;31:327–31.
14. Guo RS, Wei QT, Li HL, Wang FH. Synthesis and properties of $La_{0.7}Sr_{0.3}MnO_3$ cathode by gel combustion. Mater Lett. 2006;60:261–5.
15. Berger D, Matei C, Papa F, Macovei D, Fruth V, Deloume JP. Pure and doped lanthanum manganites obtained by combustion method. J Eur Ceram Soc. 2007;27:4395–8.
16. Mukasyan AS, Costello C, Sherlock KP, Lafarga D, Varma A. Perovskite membranes by aqueous combustion synthesis: synthesis and properties. Sep Purif Technol. 2001;25:117–26.
17. Deshpande K, Mukasyan A, Varma A. Aqueous combustion synthesis of strontium-doped lanthanum chromite ceramics. J Am Ceram Soc. 2003;86:1149–54.
18. Biamino S, Badini C. Combustion synthesis of lanthanum chromite starting from water solutions: investigation of process mechanism by DTA–TGA–MS. J Eur Ceram Soc. 2004;24:3021–34.
19. Ringuedé A, Labrincha JA, Frade JR. A combustion synthesis method to obtain alternative cermet materials for SOFC anodes. Solid State Ion. 2001;141–142:549–57.
20. Williamson GK, Hall WH. X-ray line broadening from filed aluminium and wolfram. Acta Metall. 1953;1:22–31.
21. Hwang C-C, Wu T-Y, Wan J, Tsai J-S. Development of a novel combustion synthesis method for synthesizing of ceramic oxide powders. Mater Sci Eng B. 2004;111:49–56.
22. Conceição L, Ribeiro NFP, Furtado JGM, Souza MMVM. Effect of propellant on the combustion synthesized Sr-doped $LaMnO_3$ powders. Ceram Int. 2009;35:1683–7.
23. Civera A, Pavese M, Saracco G, Specchia V. Combustion synthesis of perovskite-type catalysts for natural gas combustion. Catal Today. 2003;83:199–211.
24. Mori M, Hiei Y, Sammes NM. Sintering behavior and mechanism of Sr-doped lanthanum chromites with A site excess composition in air. Solid State Ion. 1999;123:103–11.
25. Jiang SP, Liu L, Ong KP, Wu P, Li J, Pu J. Electrical conductivity and performance of doped $LaCrO_3$ perovskite oxides for solid oxide fuel cells. J Power Sour. 2008;176:82–9.
26. Mori M, Yamamoto T, Ichikawa T, Takeda Y. Dense sintered conditions and sintering mechanisms for alkaline earth metal (Mg, Ca and Sr)-doped $LaCrO_3$ perovskites under reducing atmosphere. Solid State Ion. 2002;148:93–101.
27. Marinho EP, Souza AG, Melo DS, Santos IMG, Melo DMA, Silva WJ. Lanthanum chromites partially substituted by calcium, strontium and barium synthesized by urea combustion: thermogravimetry study. J Therm Anal Calorim. 2007;87:801–4.
28. Zupan K, Kolar D, Marinsek M. Influence of citrate–nitrate reaction mixture packing on ceramic powder properties. J Power Sour. 2000;86:417–22.
29. Rida K, Benabbas A, Bouremmad F, Peña MA, Sastre E, Martínez-Arias A. Effect of calcination temperature on the structural characteristics and catalytic activity for propene combustion of sol–gel derived lanthanum chromite perovskite. Appl Catal A. 2007;327:173–9.
30. Bansal NP, Zhong Z. Combustion synthesis of $Sm_{0.5}Sr_{0.5}CoO_{3-x}$ and $La_{0.6}Sr_{0.4}CoO_{3-x}$ nanopowders for solid oxide fuel cell cathodes. J Power Sour. 2006;158:148–53.
31. Prabhakaran K, Lakra J, Beigh MO, Gokhale NM, Sharma SC, Lal R. Sinterable $La_{0.8}Sr_{0.2}CrO_3$ and $La_{0.7}Ca_{0.3}CrO_3$ powders by sucrose combustion synthesis. J Mater Sci. 2006;41:6300–4.
32. Worayingyong A, Kangvansura P, Ausadasuk S, Praserthdam P. The effect of preparation: Pechini and Schiff base methods, on adsorbed oxygen of $LaCoO_3$ perovskite oxidation catalysts. Colloids Surf A. 2008;315:217–25.